Drug-induced modification of the system properties associated with spontaneous human electroencephalographic activity

David T. J. Liley* and Peter J. Cadusch†
Centre for Intelligent Systems and Complex Processes, School of Biophysical Sciences and Electrical Engineering, Swinburne University of Technology, Hawthorn, Victoria 3122, Australia

Marcus Gray and Pradeep J. Nathan
Brain Sciences Institute, Swinburne University of Technology, Hawthorn, Victoria 3122, Australia
(Received 8 October 2002; revised manuscript received 5 May 2003; published 24 November 2003)

The benzodiazepine (BZ) class of minor tranquilizers are important modulators of the γ-amino butyric acid ($GABA_A$)/BZ receptor complex that are well known to affect the spectral properties of spontaneous electroencephalographic activity. While it is experimentally well established that the BZs reduce total alpha band (8–13 Hz) power and increase total beta band (13–30 Hz) power, it is unclear what the physiological basis for this effect is. Based on a detailed theory of cortical electrorhythmogenesis it is conjectured that such an effect is explicable in terms of the modulation of GABAergic neurotransmission within locally connected populations of excitatory and inhibitory cortical neurons. Motivated by this theory, fixed order autoregressive moving average (ARMA) models were fitted to spontaneous eyes-closed electroencephalograms recorded from subjects before and approximately 2 h after the oral administration of a single 1 mg dose of the BZ alprazolam. Subsequent pole-zero analysis revealed that BZs significantly transform the dominant system pole such that its frequency and damping increase. Comparisons of ARMA derived power spectra with fast Fourier transform derived spectra indicate an enhanced ability to identify benzodiazepine induced electroencephalographic changes. This experimental result is in accord with the theoretical predictions implying that alprazolam enhances inhibition acting on inhibitory neurons more than inhibition acting on excitatory neurons. Further such a result is consistent with reported cortical neuronal distributions of the various $GABA_A$ receptor pharmacological subtypes. Therefore physiologically specified fixed order ARMA modeling is expected to become an important tool for the systematic investigation and modeling of a wide range of cortically acting compounds.

DOI: 10.1103/PhysRevE.68.051906 PACS number(s): 87.19.Nn, 87.19.La, 87.80.Tq, 87.18.−h

I. INTRODUCTION

γ-amino butyric acid (GABA) is the major neurotransmitter in the human brain that mediates the transmission of inhibitory events between neurons. GABA influences neurons by way of three major classes of receptors: $GABA_A$, $GABA_B$, and $GABA_C$ receptor classes. $GABA_A$ receptors are of particular interest as their function can be modulated by a wide variety of clinically relevant substances, most notably the sedative agents best exemplified by the barbiturate and benzodiazepine classes of drugs.

Benzodiazepines (BZs) are positive allosteric modulators of the $GABA_A$/BZ receptor complex. By inducing a conformational change in this receptor complex, they increase the frequency of GABA initiated channel openings. Electrophysiologically, this increased probability of channel opening is reflected in an augmentation of the amplitude and the time constant of decay of the associated unitary inhibitory postsynaptic potential (IPSP) [1,2]. Benzodiazepines have also been reported to increase single $GABA_A$ channel conductances in the presence of low synaptic concentrations of GABA [3]. Electroencephalographically benzodiazepines are well known to decrease alpha (8–13 Hz) and increase low beta (13–16 Hz) activity in a dose dependent manner [4–6]. Despite careful and thorough characterizations of the molecular pharmacology of the BZs and their various electrophysiological effects, the mechanism whereby BZs induce changes in the spectral content of the electroencephalogram (EEG) is unknown.

The recent theoretical work on the genesis of the alpha rhythm by Liley *et al.* [7–9] suggests that BZs affect the EEG by altering reverberant activity within synaptically coupled populations of inhibitory and excitatory neurons in neocortex. This theory has previously been used to investigate the mechanism of general anesthesia using substances that have been shown to alter the time course of GABA induced IPSPs [10].

This theory considers cortex as an excitable spatial continuum of reciprocally connected excitatory and inhibitory neurons interacting by way of short-range (intracortical) and long-range (cortico-cortical) connections (see Fig. 1). Because this is a theory of the genesis of the alpha rhythm, and not specifically a theory of its physiological modulation, only the time course and the corresponding reversal potentials of ''fast'' excitatory (AMPA/kainate) and ''fast'' inhibitory ($GABA_A$) neurotransmitter kinetics are explicitly incorporated. Detailed semianalytical and numerical solutions of the theory's equations have revealed a rich repertoire of physiologically plausible dynamical behavior. Of particular significance is the generation of limit cycle, chaotic, and noise

*Electronic address: dliley@swin.edu.au; http:// marr.bsee.swin.edu.au
†Electronic address: pcadusch@swin.edu.au

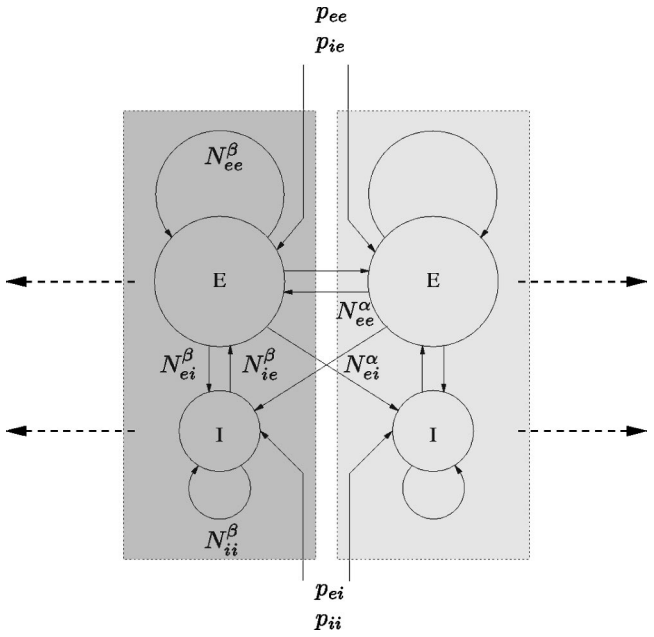

FIG. 1. Diagram illustrating the short-range (intracortical), $N_{j'j}^{\beta}$, and long-range (cortico-cortical), N_{ej}^{α}, systems that serve to connect excitatory (E) and inhibitory (I) neuronal populations in cortex. Populations that are enclosed within a dotted box correspond roughly to a cortical macrocolumn. $p_{j'j}$ denote extracortical input of type j' to neural population of type j.

driven oscillations at the frequency of the mammalian alpha rhythm, with model parameters that are all within ranges reported experimentally [8,11].

Loosely speaking, such oscillatory activity in the EEG is theorized to arise from oscillatory activity occurring simultaneously in local inhibitory→inhibitory circuits and local inhibitory→excitatory→inhibitory circuits. Oscillations generated by inhibitory→inhibitory circuits are predicted to have a higher frequency than those generated in inhibitory→excitatory→inhibitory circuits because the total loop delay of the former (t_{ii}^{p}) is less than the loop delay of the latter ($t_{ie}^{p}+t_{ei}^{p}$) as $t_{ii}^{p} \leqslant t_{ie}^{p}$. These loop delays will correspond respectively to the mean times to peak for excitatory postsynaptic potentials (EPSPs) and IPSPs induced in the dendrites of excitatory and inhibitory neurons when measured at the soma. Thus strengthening inhibitory→excitatory population connectivity will weight the EEG toward lower frequencies, whereas strengthening inhibitory→inhibitory connections will weight the EEG toward higher frequencies.

On this basis it is hypothesized that benzodiazepines shift the alpha to higher frequencies because they amplify inhibitory→inhibitory population synaptic interactions to a greater degree than inhibitory→excitatory interactions. To test this hypothesis eyes-closed EEGs were recorded from subjects who had taken a low dose of a short acting benzodiazepine, alprazolam. The EEGs was then analyzed using theoretically motivated fixed order autoregressive moving average (ARMA) time series modeling. Our results provide strong experimental evidence for interpreting benzodiazepine induced electroencephalographic changes as due to the modulation of a cortical white noise filter.

II. THEORY

The alpha rhythm is arguably the most obvious recordable feature of the intact human brain. While the exact basis for its genesis is still controversial it is widely believed that it arises as a consequence of one or more of the following mechanisms: endogenous or exogenous (thalamic) pacing of cortical neurons [12–14]; oscillatory activity generated through the reciprocal feedforward interactions of excitatory (pyramidal) and inhibitory (interneuron) cortical neuronal populations [15–18]; or boundary dependent standing wave generation (Schumann resonance-like) due to long-range cortico-cortical connectivity [19–21]. The theory of Liley *et al.* [7–9], however, suggests that none of these mechanisms are sufficient, either separately or taken together, in explaining the physiological genesis of the alpha rhythm.

In this theory it is found that the strength and form of population inhibitory→inhibitory synaptic interactions are the most important determinants of the frequency and damping of the emergent theoretical alpha band oscillatory activity. Such behavior arises principally because local inhibitory→inhibitory and local inhibitory→excitatory loop delays that are associated with physiologically and electroencephalographically plausible alpha activity are longer than the corresponding local (intracortical) and long-range (cortico-cortical) excitatory-excitatory loop delays. It is important to emphasize that the predicted importance of local circuit inhibitory→inhibitory population activity in the genesis of alpha band activity *emerges* from a theory in which both local (intracortical) and global (cortico-cortical) neuronal circuit activity have been incorporated.

The theory considers the EEG and ECoG (electrocorticogram) as being linearly related to the mean (over a spatial scale of the order of approximately 1 mm) soma membrane potential of underlying cortical excitatory (pyramidal) neurons $[h_e(x,t)]$. It differs from other macroscopic continuum theories [19,21–23] in that the time course of the unitary IPSP is described by a third-order differential equation. Lower orders are theoretically found unable to support any appreciable or widespread alpha band activity. Appendix A contains further details. Like other rate based theories of electrocortical activity [15,17,24], oscillatory activity in the EEG is posited to correspond to periodic modulations in the average neuronal firing rate and *not* to the average firing frequency of excitatory neurons. This continuum *mean firing rate based* theory is ''mechanistically'' quite distinct from the discrete *spike based* inhibitory interneuron network models that have been developed to investigate the genesis of synchronized gamma activity [25]. Of particular note is that these spike based interneuron network models predict that benzodiazepines will be associated with *reductions* in the frequency of the dominant γ band (40 Hz) population oscillations [25].

The intuitive basis for interneuron oscillations in this theory is as follows (see Fig. 2). Initially activated inhibitory neurons (due to constant extra-/intracortical excitatory input) give rise to inhibitory neural firings which, after a single loop

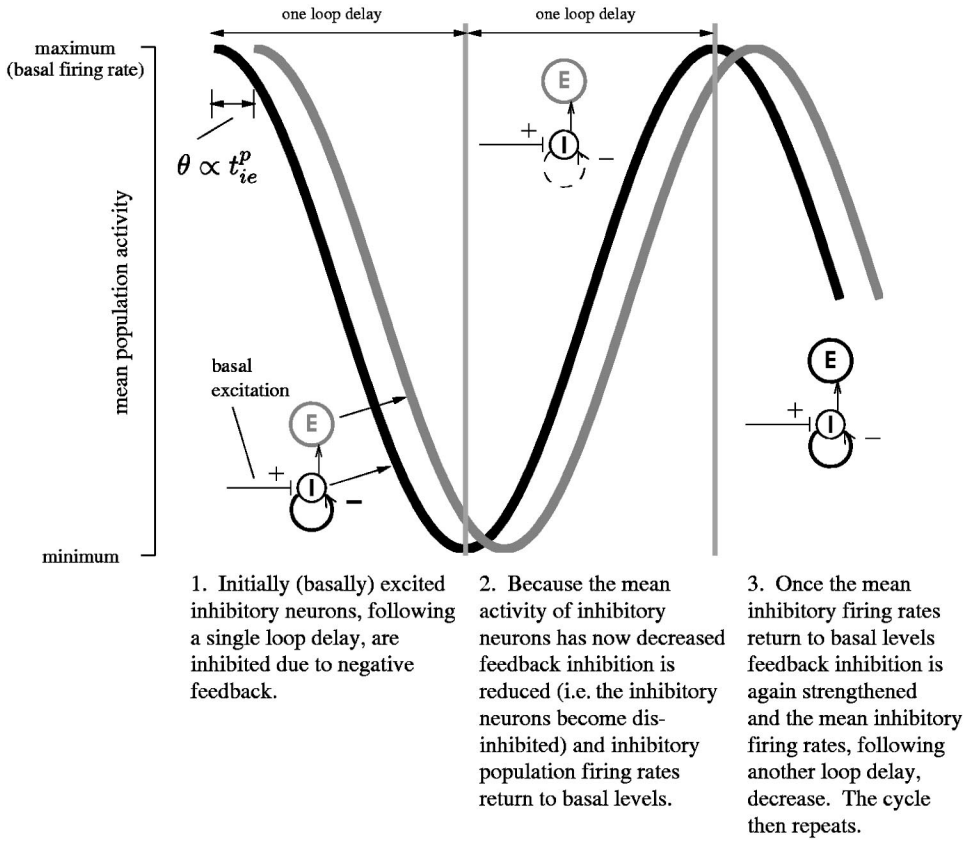

FIG. 2. Oscillatory activity generated by negative feedback within cortical interneuron (inhibitory) circuits is hypothesized to be the basis for rhythmic activity within the alpha band (8–13 Hz). Inhibitory population activity is predicted to phase lead excitatory population activity by an amount proportional (θ) to the mean inhibitory→excitatory loop delay t_{ie}^{p} (i.e., mean time to peak for an IPSP induced in an excitatory neuron when measured at the soma). *E* and *I* refer to local cortical populations of excitatory and inhibitory neurons, respectively. The excitatory→excitatory and excitatory→inhibitory connections of Fig. 1 have been omitted for clarity.

delay (t_{ii}^{p}), feed back to inhibit and thereby reduce the activity of these initially active inhibitory neurons. Because the activity of this inhibitory neural population is now reduced, the inhibitory population feedback is subsequently weakened and thus, after another loop delay, inhibitory population activity again increases, and thus the previous sequence of events can start anew. In this manner oscillations are generated with a period of $O(t_{ii}^{p})$.

Such inhibitory local circuit activity is made experimentally observable by coupling to the adjacent population of excitatory neurons. Thus it is predicted that inhibitory population activity will *phase lead* excitatory population activity by an amount proportional to the mean inhibitory →excitatory loop delay (t_{ie}^{p}). This, as yet experimentally untested, prediction serves to distinguish our hypothesized mechanism of EEG rhythmogenesis from those posited by other workers (e.g., Freeman [26]).

Theoretical predictions

From a mathematical point of view the theory's equations are cast as a coupled set of nonlinear partial differential equations (see Appendix A). Explicit quantitative solutions to these equations can be obtained only through numerical integration as analytical solutions do not exist. Fortunately, many important qualitative properties of these equations can be understood through linearization. Linearization of these equations about a singular point yields the following linear time invariant system:

$$H_e(k,\omega) = G_e(k,\omega,q)P(k,\omega) \tag{1}$$

$$= \frac{N(k,\omega,q)}{D(k,\omega,q)}P(k,\omega) \tag{2}$$

$$= \frac{\sum_{m=0}^{5} b_m(k,q)\omega^m}{\sum_{n=0}^{8} a_n(k,q)\omega^n} P(k,\omega), \tag{3}$$

where k and ω are the wave number and angular frequency, respectively. Loosely speaking, k specifies the reciprocal of the characteristic physical scale over which oscillations of frequency ω occur. Based on theoretical and numerical arguments (Appendix B), we are able to set k to a fixed value of 0.4 rad cm^{-1} for all ω. $H_e(k,\omega)$ is the Fourier transform of the *mean soma membrane potential of excitatory neurons* $h_e(x,t)$, G_e is the *electrocortical transfer function*, q is a

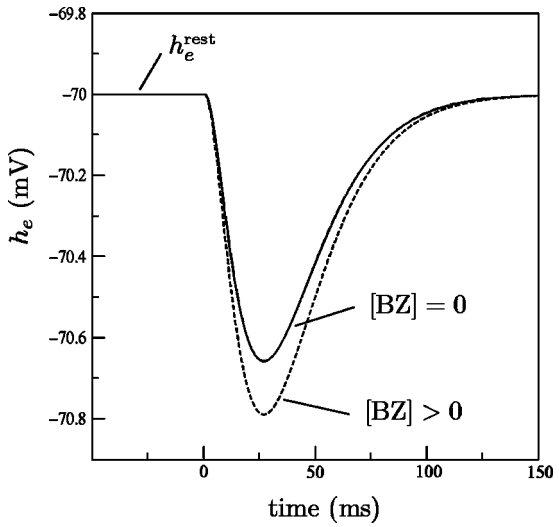

FIG. 3. A schematic diagram summarizing the essential experimental effect of nonzero extracellular benzodiazepine levels ([BZ]) in augmenting the amplitude of the unitary inhibitory postsynaptic potential induced in an excitatory neuron. The respective IPSPs are induced by a presynaptic spike arriving at $t=0$ in a neuron at rest. h_e and h_e^{rest} are the *mean* and *mean resting soma membrane potentials*, respectively, of excitatory cortical neurons. These particular IPSPs were numerically calculated from the theory of Liley *et al.* [8]. See Appendix A and Eqs. (A7)–(A8) for further details.

vector of parameters, and $P(k,\omega)$ represents the spatiotemporal form of cortical input. The theory includes such parameters as EPSP and IPSP potential peak amplitudes and time courses, neuronal membrane time constants, excitatory and inhibitory population connectivities, as well as physiologically derived functions specifying mean neuronal population firing rates as a function of the respective mean soma membrane potentials.

In the absence of any information to the contrary, it is assumed that the cortical input $P(k,\omega)$ is spatiotemporally so complicated as to be indistinguishable from band limited white noise [8,17,20,24,27,28]. On this basis, solutions to $D(k,\omega)=0$ for fixed real k give the theoretically predicted EEG resonant frequencies. The interesting interpretation of this result is that the eyes-closed mammalian alpha rhythm arises because cortex acts as a white noise filter to its input. In discrete time signal processing Eq. (3) can be modeled by an ARMA model of MA order max(m)=5 and AR order of max(n)=8 if $P(k,\omega)$ is Gaussian noise [29]. These orders correspond to the respective polynomial orders of the denominator and numerator of the theoretically derived electrocortical transfer function [Eq. (3) and Eqs. (A10)–(A13) in Appendix A].

In general, no analytical results can be obtained for the roots of $D(k,\omega)$ and thus the functional dependence of these roots (also known as poles) on physiological and anatomical parameters cannot be explicitly obtained. However, by performing a Monte Carlo parameter space search (assuming all parameters are uniformly distributed over physiologically plausible ranges) (see Table IV below and [8] for further details), sets of parameters can be found that give rise to electroencephalographically plausible eyes-closed alpha activity ($f_c/\Delta f_{\text{FWHM}} \geqslant 5$ for a spectral f_c peak lying between 8 and 13 Hz). The sensitivity of these alpha resonances to systematic parametric perturbations can be determined analytically [8]. Given that benzodiazepines are known to augment the amplitude of GABA mediated IPSPs (Fig. 3) it is to be expected that all inhibitory population synaptic connections will be strengthened. Therefore the sensitivity of these theoretical resonances to variations in N_{ii}^{β} (inhibitory→inhibitory population connection strength) and N_{ie}^{β} (inhibitory→ excitatory population connection strength) is of particular rel-

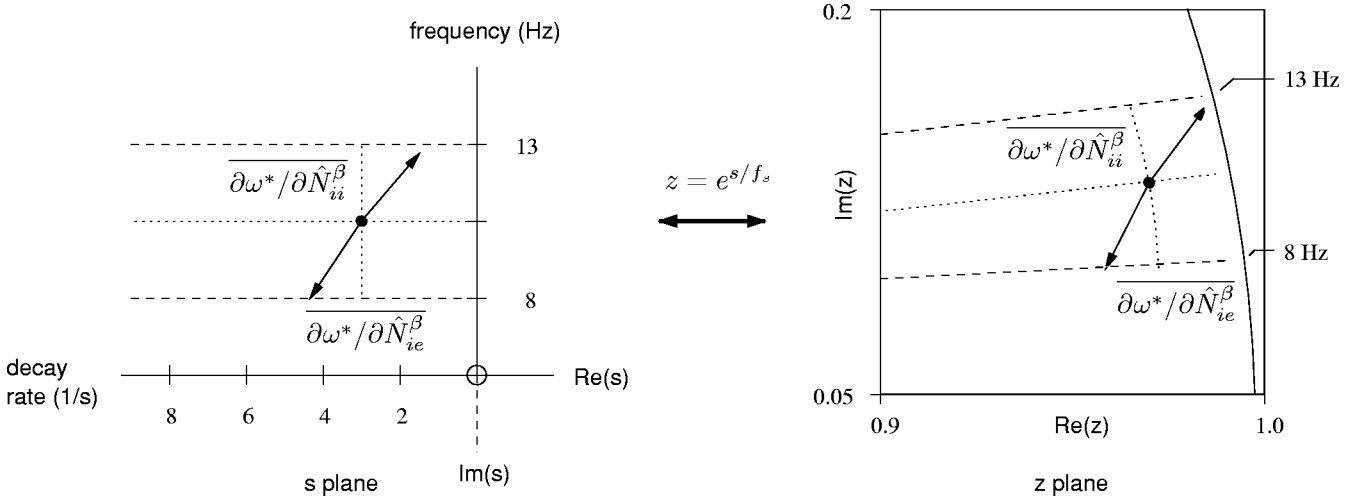

FIG. 4. Schematic representation of the predicted effects of increasing the strength of neuronal population inhibitory-inhibitory and inhibitory-excitatory synaptic interactions assuming that scalp EEG activity has a characteristic physical scale of $k=0.4$ rad cm^{-1}. The filled circle approximately represents the theoretical loci of the dominant poles associated with electroencephalographically plausible eyes-closed alpha activity. The arrows indicate the mean predicted direction of motion of these poles in response to increases in inhibitory→inhibitory ($\overline{\partial\omega^*/\partial\hat{N}_{ii}^{\beta}}$) and inhibitory→excitatory ($\overline{\partial\omega^*/\partial\hat{N}_{ie}^{\beta}}$) synaptic strength. Equivalent s plane (Laplace or Fourier plane) and z plane representations are shown. Decay rates are shown increasing to the left as they correspond to Re(s)<0 (i.e., the negative real half of the s plane). For illustrative purposes indicated changes are not to scale. See Sec. II A and Table I for full details.

TABLE I. Mean sensitivities of model alpha activity to increases in inhibitory-inhibitory (N_{ii}^{β}) and inhibitory-excitatory (N_{ie}^{β}) synaptic strength for a variety of wave numbers (characteristic physical scales). Results are not shown for $k=0$ as this implies an infinite characteristic physical scale for the theoretical alpha. We have theoretically assumed that the characteristic scale of scalp recorded EEGs corresponds to $k \approx 0.4$ rad cm^{-1} (see Appendix B). Results shown for each k were calculated from 2000 parameter sets found to support electroencephalographically plausible alpha. For further details see the Appendix A and [8].

k (rad cm^{-1})	$\overline{\frac{\partial \mathrm{Re}(\omega^*)}{\partial \hat{N}_{ii}^{\beta}}}$ (rad s^{-1})	$-\overline{\frac{\partial \mathrm{Im}(\omega^*)}{\partial \hat{N}_{ii}^{\beta}}}$ (s^{-1})	$\overline{\frac{\partial \mathrm{Re}(\omega)^*}{\partial \hat{N}_{ie}^{\beta}}}$ (rad s^{-1})	$-\overline{\frac{\partial \mathrm{Im}(\omega)^*}{\partial \hat{N}_{ie}^{\beta}}}$ (s^{-1})
0.2	0.03	43.1	1.1	−80.5
0.4	19.1	30.2	−28.5	−58.2
0.6	32.0	−3.7	−47.4	−2.9
0.8	36.2	−24.3	−54.0	34.3
1	39.2	−33.6	−58.6	42.2
2	43.0	−156.3	−64.4	226.0
15	47.8	−167.0	−69.7	240.0

evance. Figure 4 and Table I details these theoretical predictions for a range of wave numbers. It is found that increases in N_{ii}^{β} are predicted to increase the frequency of the alpha whereas increases in N_{ie}^{β} are predicted to decrease frequency for all values of k.

It is useful to compare predictions made by other competing theories of alpha electrorhythmogenesis of the effects of benzodiazepines on EEG dynamics. Table II outlines the predicted effects of benzodiazepines on the change in relative alpha (8–13 Hz) and beta (13–30 Hz) spectral powers. The theory of Liley *et al.* [7–9] is currently the only one to make predictions that are consistent with the known effects of benzodiazepines on the EEG.

Specifically, it is hypothesized that

$$\Delta\omega^* = \mu\left(\epsilon\frac{\partial\omega^*}{\partial\hat{N}_{ii}^{\beta}} + \frac{\partial\omega^*}{\partial\hat{N}_{ie}^{\beta}}\right)[\mathrm{BZ}], \tag{4}$$

where μ and ϵ are real constants, [BZ] is the extracellular benzodiazepine concentration, and $\Delta\omega^*$ (which will be complex) is the corresponding change in pole location in the complex Fourier plane. $\partial\,\mathrm{Re}(\omega^*)/\partial\hat{N}_{ii}^{\beta}$ and $\partial\,\mathrm{Re}(\omega^*)/\partial\hat{N}_{ie}^{\beta}$ provide local measures of how sensitive the frequency of the model alpha is to unit normalized changes in N_{ii}^{β} and N_{ie}^{β}, respectively. $-\partial\,\mathrm{Im}(\omega^*)/\partial\hat{N}_{ii}^{\beta}$ and $-\partial\,\mathrm{Im}(\omega^*)/\partial\hat{N}_{ie}^{\beta}$ provide local measures of how sensitive the damping of the model alpha is to unit normalized changes in N_{ii}^{β} and N_{ie}^{β}, respectively. The corresponding motion in the s and z planes is $\Delta s^* = i\Delta\omega^*$ and $\Delta z^* = e^{i\Delta\omega^*/f_s}$, respectively (where f_s is the sampling frequency in hertz). ϵ is the relative pharmacological potency of alprazolam acting at GABA_A receptors on inhibitory neurons compared to alprazolam acting at GABA_A receptors on excitatory neurons. Thus $\epsilon\mu[\mathrm{BZ}]$ and $\mu[\mathrm{BZ}]$ are the fractional changes in the mean peak amplitudes of IPSPs effected by benzodiazepines in inhibitory and excitatory neural populations, respectively. See Appendix A and Eq. (A22) for further details.

TABLE II. Predicted changes in *relative* alpha ($\Delta\alpha$) and beta ($\Delta\beta$) spectral powers following benzodiazepine administration for all the major theories of alpha electrorhythmogenesis.

Theory	Refs.	$\Delta\alpha$	$\Delta\beta$
Liley *et al.*	[8,9]	−	+
Classical pacemaker/spindle rhythm (reticular thalamic)	[30,31]	−	−
Thalamocortical circuit rhythm	[32,33]	−	−
Spike based interneuron network	[25,34]	+/0	+
Reciprocally connected excitatory and inhibitory population	[16,17]	+	−

We note that Eq. (4) enables estimates of ϵ and μ [BZ] to be obtained from experimental data. By solving this simultaneous equation we obtain

$$\epsilon = \frac{\mathrm{Im}(\partial\omega^*/\partial N_{ie}^{\beta}\overline{\Delta\omega^*})}{\mathrm{Im}(\overline{\partial\omega^*/\partial N_{ii}^{\beta}}\Delta\omega^*)}, \tag{5}$$

$$\mu[\mathrm{BZ}] = \frac{\mathrm{Im}(\partial\omega^*/\partial N_{ii}^{\beta}\overline{\Delta\omega^*})}{\mathrm{Im}(\partial\omega^*/\partial N_{ii}^{\beta}\overline{\partial\omega^*/\partial N_{ie}^{\beta}})}, \tag{6}$$

where the overbar in this equation represents the complex conjugate.

III. METHODS AND MATERIALS

A. Subjects

In a randomized, placebo-controlled, double-blind two-way crossover study, 18 healthy male nonsmokers were investigated. Females were not recruited as contraceptive and menstrual effects are known to affect the expression of eyes-closed alpha activity and to alter benzodiazepine sensitivity [35,36]. Further, it is known that a variety of steroid hormones (including endogenous progesterone) are able to modulate GABA physiologic responses and hence benzodi-

azepine sensitivity. Subjects were recruited via university notice board advertisements. Subjects were randomized using a simple randomization procedure after screening tests were performed. All subjects were drug-free and in good health as determined by a complete physical examination. Each subject gave written informed consent before taking part in the study, which was approved by the Human Research Ethics Committee of the Swinburne University of Technology.

B. Study design

On the day of testing, subjects randomly received either a placebo or alprazolam 1 mg (Xanax, Pharmacia Australia) as a single oral dose. Alprazolam was chosen for three principal reasons: (i) plasma levels of any psychoactive metabolites are extremely low, (ii) it has a relatively short elimination half-life ($t_{1/2}=6-19$ h), and (iii) it has a relatively rapid time to peak following oral administration ($t_{\text{peak}}=1-2$ h) [4]. All testing sessions were separated by at least 1 week to allow for drug washout. On the morning of each recording session subjects received a light breakfast. Baseline EEG recordings were then taken prior to drug/placebo administration. 75 min after taking the drug/placebo subjects received a light lunch. Approximately 30 min following this subjects then commenced postdrug/placebo EEG recordings.

C. EEG recording

Before taking the randomly assigned medication all subjects underwent a baseline EEG recording consisting of approximately 66 s each of spontaneous EEG recorded under the following conditions: eyes closed relaxing, eyes closed mental subtraction, eyes open relaxing, and eyes open mental subtraction. Subjects then underwent an identical set of recordings two hours after receiving the medication. Following this, subjects underwent further tests that were of no importance to this study.

All EEG recordings were performed using custom built amplifiers, A/D conversion, and serial data collection developed by the Brain Sciences Institute of Swinburne University of Technology. The EEG was recorded referenced to linked ears using 64 scalp electrodes attached to an electrode cap using the nasion as a ground. Electrodes were positioned according to the international 10:20 standard system with the addition of midpoint electrodes. Because of the occipital dominance of the alpha rhythm, only an occipital electrode subset was analyzed. In particular, EEGs recorded from electrode 48 (midway between Pz and P3), electrode 50 (midway between Pz and P4), electrode 56 (midway between Pz and O1), and electrode 57 (midway between Pz and O2) were analyzed. The EEG was bandpass filtered (0.1–80 Hz) and sampled at 500 Hz (f_s).

D. Data analysis

All data were archived on CD for subsequent analysis. After the removal of nonfunctioning electrodes, each 66 s spontaneous EEG channel recording was optimally (Wiener) filtered using a 201 point LMS (least mean square) adaptive filter to remove periodic 50 Hz interference, which is known to compromise subsequent ARMA coefficient estimation. Such filtering was preferred to an *a priori* fixed coefficient digital low-pass or bandpass filter as it is better suited to the removal of a periodic artifact in a nonstationary signal. Each filtered 66 s recording was decomposed into 50% overlapping 1024 point ($\approx$2 s) segments for ARMA modeling. After the mean was removed each 2 s epoch was fitted with an (8,5) order ARMA model (ARMASA Matlab Toolbox) [37,38]. Formally, each EEG segment $y(n)$ based on Eq. (3) was modeled as

$$y(n)=-\sum_{k=1}^{8} a_k y(n-k)+\sum_{k=0}^{5} b_k u(n-k), \tag{7}$$

where $u(n)$ is assumed to be a white noise (Gaussian) process. By taking the z transform this can be written equivalently in the z domain as

$$Y(z)=\frac{\sum_{k=0}^{5} b_k z^{-k}}{1+\sum_{k=1}^{8} a_k z^{-k}}\ U(z)=\frac{B(z)}{A(z)}\ U(z). \tag{8}$$

Solutions to $A(z)=0$ will give the system poles and solutions to $B(z)=0$ give the system zeros. In general these solutions are complex with $|z|<1$. Assuming a single dominant weakly damped pole, z_0 ($|z_0|\approx 1$), $f_s\,\text{Arg}(z_0)/2\pi$ is the frequency and

$$\gamma \approx f_s \frac{1-|z_0|}{\sqrt{|z_0|}} \tag{9}$$

the damping of the dominant temporal mode constitutive of the alpha resonance. f_s is the sampling frequency. Note that as $|z_0|\to 1$, $\gamma\to 0$, and as $|z_0|\to 0$, $\gamma\to\infty$, as consistency demands.

For each session involving placebo (PL) or benzodiazepine the difference in the average location of poles (determined for each 2 s segment) lying between 6 and 30 Hz before ($-$) and after ($+$) the administration of either the PL or BZ was calculated for each subject and channel, i.e.,

$$\Delta\theta_{\text{PL}}=\text{Arg}(\langle z_0\rangle_{\text{PL}+})-\text{Arg}(\langle z_0\rangle_{\text{PL}-}), \tag{10}$$

$$\Delta r_{\text{PL}}=|\langle z_0\rangle_{\text{PL}+}|-|\langle z_0\rangle_{\text{PL}-}|, \tag{11}$$

$$\Delta\theta_{\text{BZ}}=\text{Arg}(\langle z_0\rangle_{\text{BZ}+})-\text{Arg}(\langle z_0\rangle_{\text{BZ}-}), \tag{12}$$

$$\Delta r_{\text{BZ}}=|\langle z_0\rangle_{\text{BZ}+}|-|\langle z_0\rangle_{\text{BZ}-}|. \tag{13}$$

For each channel the following null hypotheses were evaluated using a distribution-free paired one-sided permutation (resampling) test [39]:

$$\text{H}_0:\quad \overline{\Delta\theta_{\text{BZ}}}\leqslant\overline{\Delta\theta_{\text{PL}}}, \tag{14}$$

$$\text{H}_0:\quad \overline{\Delta r_{\text{BZ}}}\geqslant\overline{\Delta r_{\text{PL}}}. \tag{15}$$

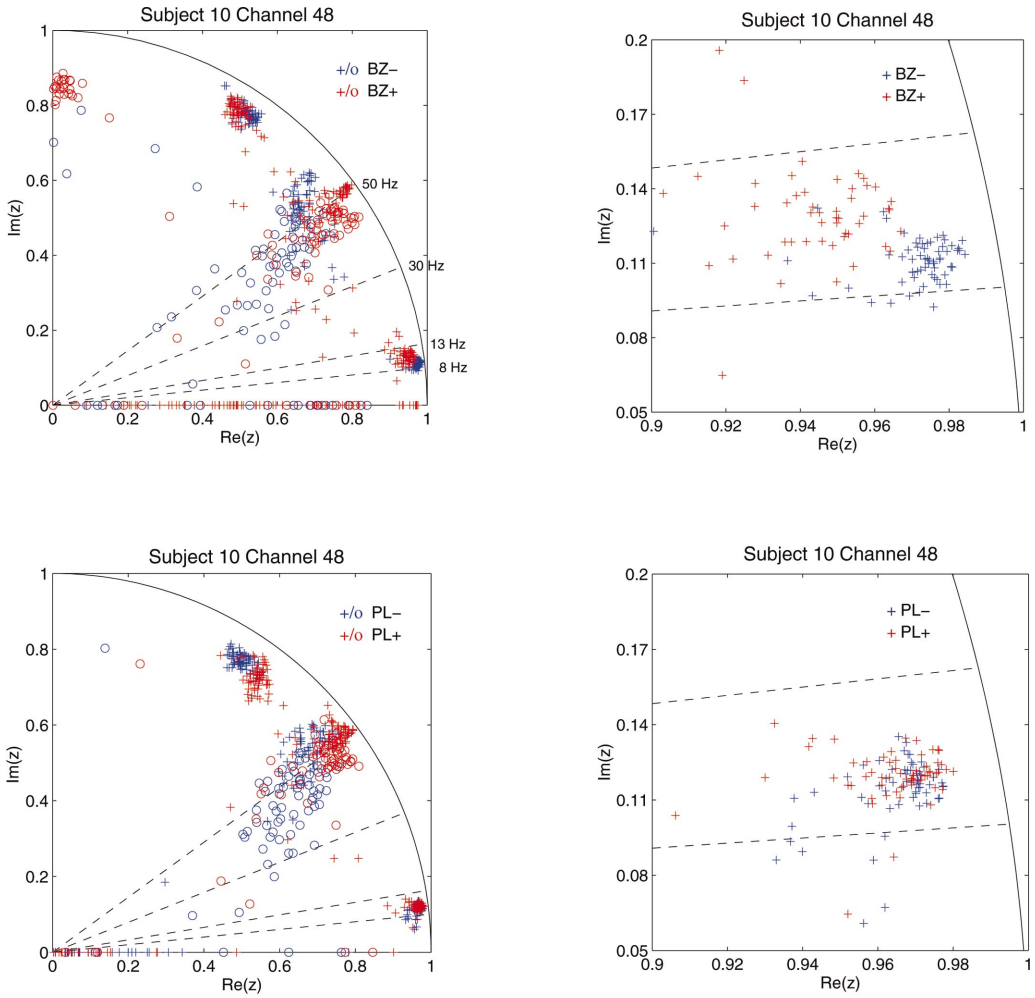

FIG. 5. (Color) Pole-zero plot of the upper right quadrant of the z plane for a typical subject for the BZ−/BZ+ condition (top two figures) and the PL−/PL+ condition (bottom two figures). Note the distinct populations of poles (+) and zeros (○) (left hand figures). Right hand figures show in more detail the region of the z plane corresponding to 8–13 Hz activity. Differences between both r and θ of the BZ− and BZ+ alpha pole centroids are highly significant ($p \ll 0.001$). The upper left quadrant of the z plane has not been plotted as it contains no poles of electroencephalographic relevance and the lower half of the complex z plane has been omitted as it is the mirror image of the upper half.

For each subject and electrode ARMA power spectra $[|B(e^{i\omega})/A(e^{i\omega})|^2]$ were calculated for all 2 s segments and then averaged. Similarly, for each subject and electrode fast Fourier transform FFT power spectra were calculated for all 50% overlapping 2 s segments and then averaged. In both cases the location of the spectral peak (f_c) in between 8 and 13 Hz was determined as were the relative (to the total power over the interval 0–30 Hz) alpha (8–13 Hz) and beta (13–30 Hz) powers.

IV. RESULTS

Of the 18 subjects recruited, one did not complete the study, two did not display a clear eyes-closed resting alpha rhythm, and another became quite drowsy following oral benzodiazepine administration. For these subjects the associated data were eliminated from the subsequent data analysis. For one of the remaining subjects, electrode 56 in the BZ+ condition did not yield a viable EEG signal and thus was not included in any further analysis.

A. Intrasubject differences

Figure 5 illustrates the results of a typical ARMA based pole-zero analysis before and after an oral dose of alprazolam. The important features to note are (i) the distinct groupings of poles and zeros populating the z plane, (ii) distinct populations of poles having frequencies lying in the range 8–13 Hz, (iii) clear differences between the location of the centroids of the alpha poles before (BZ−) and following (BZ+) benzodiazepine, (iv) insubstantial differences between the location of the alpha poles before (PL−) and following (PL+) placebo, and (v) zeros at approximately 50 Hz due to the adaptive removal of mains interference and poles at about 80 Hz corresponding to the band edges of the low-pass analog filtering. In this example it is evident that the variability ($\overline{|z_0 - \langle z_0 \rangle|}$) in alpha pole location after the ingestion of the benzodiazepine is more pronounced than in the other three conditions. Further, the mean of this variability over all subjects and electrodes is significantly greater ($p = 0.0443$) in the BZ+ condition compared to the BZ− condition.

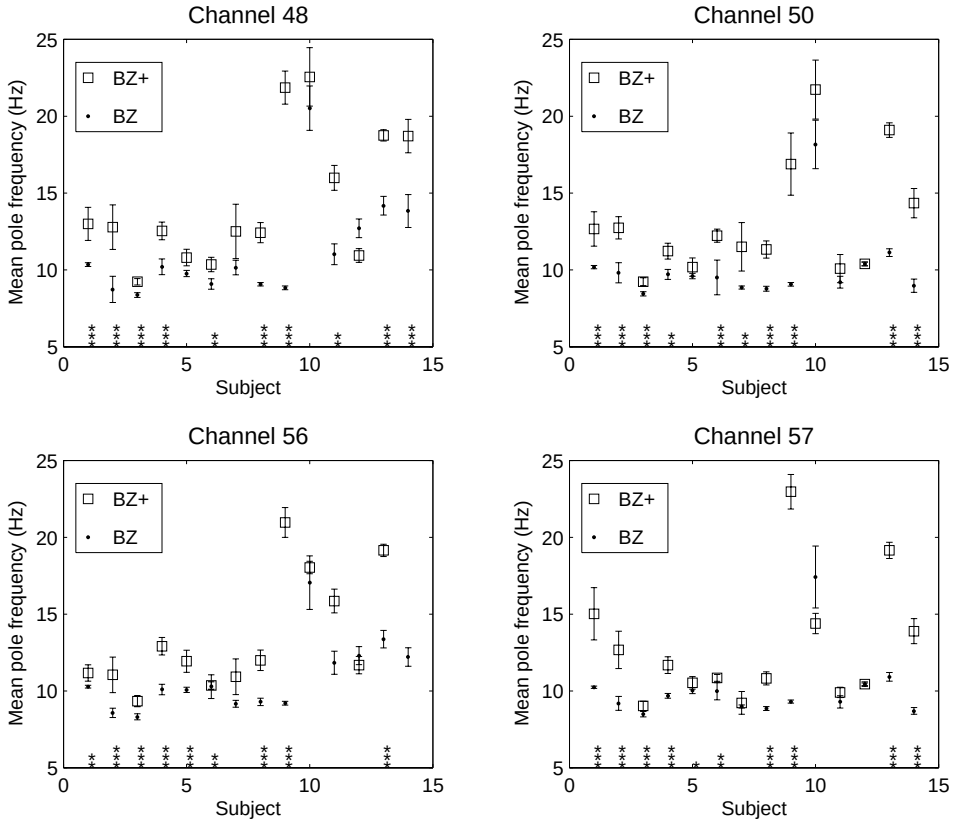

FIG. 6. Mean pole frequency ± one standard error in the mean for all poles lying between 6 and 30 Hz for each subject, before (BZ−) and after (BZ+) alprazolam administration. The significance level (i.e., the probability p of a type I error) associated with an increase in the mean pole frequency following BZ administration is indicated just above the abscissa: no stars, not significant; *, $0.01<p\leqslant 0.05$; **, $0.001<p\leqslant 0.01$; ***, $p\leqslant 0.001$. The p values for each subject and condition were determined by treating each of the 2 s epochs for that subject and condition as a sequence of independent samples. The p values were calculated using 10^6 permutations in an unpaired one-sided permutation test which preserved the number of entries in before (BZ−) and after (BZ+) conditions as well as automatically allowing for the problem of multiple comparisons over the four electrodes used. The values are thus experimentwise p values and are assigned to electrodes in a way that avoids the need for a Bonferroni correction (or some such) when interpreting the significance levels. The error bars are ± one standard error in the mean, estimated from the epochs for each subject and electrode and corrected for correlations between near neighbor epochs.

Figures 6 and 7 present a summary of the differences in pole location before and after benzodiazepine administration for each subject and electrode. Figure 6 indicates that an increase in the mean pole frequency (over the range 6–30 Hz) following benzodiazepine administration occurred in up to 13 of 14 subjects. Such a shift was significant at the $p\leqslant 0.001$ level in at least one of the four electrodes for 10 subjects. Figure 7 indicates that an increase in the mean pole damping (for poles in the range 6–30 Hz) following benzodiazepine administration occurred in up to 12 of 14 subjects. Such a shift was significant at the $p\leqslant 0.001$ level in at least one of the four electrodes for eight subjects.

By comparison, the mean pole frequency and mean pole damping increased significantly ($p\leqslant 0.001$) in only three of 14 subjects (results not shown) following placebo administration, with the magnitude of these shifts being less than in the corresponding benzodiazepine condition.

B. Population differences

Figure 8 illustrates the difference in the average location of poles (determined for each 2 s segment) lying between 6 and 30 Hz before (−) and after (+) the administration of either the PL or BZ, for each subject and channel. For the placebo condition intersubject variations in $\Delta\theta$ and Δr are centered about (0,0), whereas the corresponding variations for alprazolam are centered about a point in the lower right quadrant of the $\Delta\theta$-Δr plane. There was no inferrable relationship between θ and $\Delta\theta$ or r and Δr. For all electrodes $\Delta\theta$ for the BZ condition was significantly greater than $\Delta\theta$ for the PL condition, i.e., the null hypothesis of Eq. (14) was rejected. For all but one electrode, Δr for the BZ condition was significantly more negative than Δr for the PL condition, i.e., the null hypothesis of Eq. (15) was rejected. It is interesting to note that these differences between PL and BZ conditions are more significant for the anterior electrodes (48 and 50) than the posterior electrodes (56 and 57). However, while the mean frequency shift of the alpha pole was greater in the anterior electrodes (3.14 Hz) than in the posterior pair (2.76 Hz), this difference was not significant ($p=0.2535$).

Figure 9 illustrates the pooled data for all subjects and electrodes for both the placebo and benzodiazepine condi-

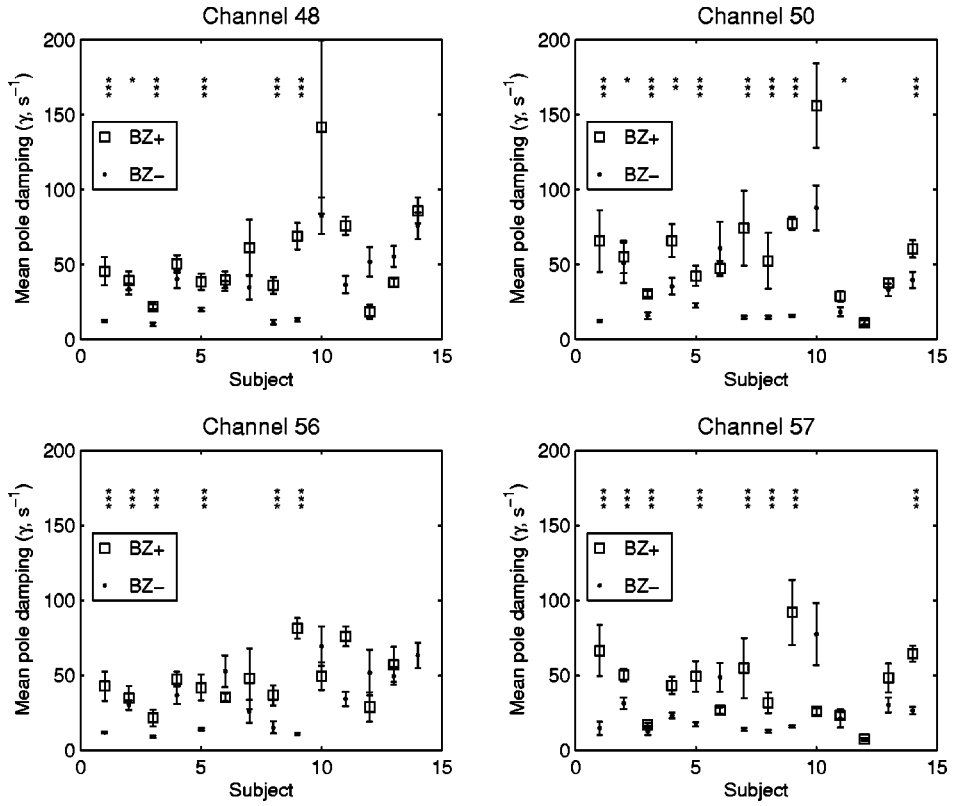

FIG. 7. Mean pole damping ± one standard error in the mean for all poles lying between 6 and 30 Hz for each subject, before (BZ−) and after (BZ+) alprazolam administration. The significance level (i.e., the probability p of a type I error) associated with an increase in mean pole damping following BZ administration is indicated at the top of each figure: no stars, not significant; *, $0.01<p\leqslant 0.05$; **, $0.001<p\leqslant 0.01$; ***, $p\leqslant 0.001$. p values and error bars were calculated in the same manner as the mean pole frequencies of Fig. 6.

tions. Of note is the clear difference in the distributions of pole frequencies and pole dampings between the two conditions. Following benzodiazepine administration both median pole frequency and median pole damping have increased.

C. Comparisons between parametric and nonparametric methods

Table III shows the results of comparisons between the parametric ARMA methods used here and the better known nonparametric Fourier methods. Each method was used to calculate (i) the mean difference in the alpha center frequency, (ii) the mean difference in relative alpha power, and (iii) the mean difference in relative beta power between PL and BZ conditions. In all cases the results obtained based on the ARMA spectra were comparable to those obtained from periodogram analysis. In particular, both methods consistently indicated opposite motions in the alpha center frequency f_c for the BZ condition when compared to the PL condition. Except for electrode 50 the changes in the alpha center frequency Δf_c were not significant. In spite of this, both methods indicated significant and substantial differences in relative alpha and beta power following alprazolam. In all cases, relative alpha power decreased while relative beta power increased. It is noteworthy that these differences were almost invariably more significant when the ARMA method was used.

V. DISCUSSION

The resting alpha rhythm is theoretically hypothesized to arise as a result of the filtering of input signals to cortex. The filter properties are determined by the bulk (macroscopic/large-scale) anatomical and physiological properties of excitatory and inhibitory cortical neurons. In this theory inhibition is conceived as having an important role in determining the properties of this ''cortical filter'' and thereby the spectra of the alpha rhythm. In particular the selective modification of the strength of cortical inhibitory action by benzodiazepines such as alprazolam is predicted to be associated with quite specific changes in the properties of this filter.

Compared to the placebo condition, it was found that alprazolam causes a significant shift in the most weakly damped pole constituting the alpha rhythm, such that its corresponding frequency and damping both increased. In the absence of any other poles this implies that alprazolam causes the alpha spectrum to shift to the right and broaden. However, in general, a pole also exists having zero frequency and finite damping (i.e., the pole is on the negative real s axis; see Fig. 4 and the top left panel of Fig. 5) which complicates such a simple interpretation, thus making it difficult to use nonparametric spectral methods (see Table III) to quantify alpha center frequency (f_c) and spectral width (e.g., full width half maximum). However, the motion of this single pole (actually a pair of conjugate poles) would be associated with a reduction in alpha band power and an in-

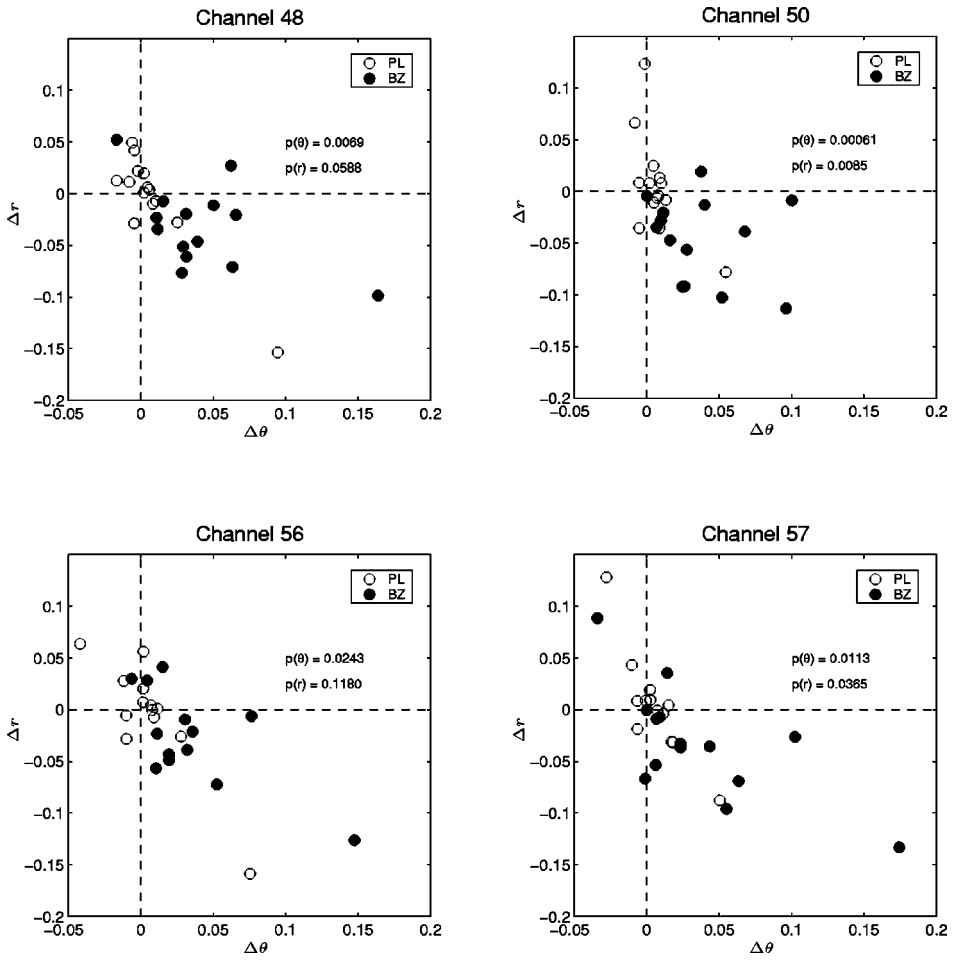

FIG. 8. $\Delta\theta$ and Δr [see Eqs. (10)–(13)] for channels 48, 50, 56, and 57. Open circles indicate the PL condition and closed circles represent the BZ condition for each of the 14 subjects. $p(\theta)$ and $p(r)$ give the significance levels, as determined by a one-sided permutation test, for the rejection of the null hypotheses $\overline{\Delta\theta_{\mathrm{BZ}}} \leqslant \overline{\Delta\theta_{\mathrm{PL}}}$ [Eq. 14)] and $\overline{\Delta r_{\mathrm{BZ}}} \geqslant \overline{\Delta r_{\mathrm{PL}}}$ [Eq. (15)].

crease in beta band power. The results of calculating the corresponding ARMA spectra (see Table III) are consistent with this and are entirely comparable to those obtained using the more commonly used and better known nonparametric Fourier methods. Theoretically based ARMA modeling of the electroencephalographic effects of benzodiazepines provides additional information that cannot be obtained from the model-free empirical approaches exemplified by Fourier spectral analysis.

On the basis of the theory small changes in inhibitory→inhibitory and inhibitory→excitatory population coupling strength typically have opposite effects on the most weakly damped pole constitutive of alpha. Increases in N_{ii}^{β} were predicted to increase the frequency and damping of such a pole, whereas increases in N_{ie}^{β} were predicted to decrease the frequency and damping. These predictions coupled with our experimental results lead us to conclude that alprazolam increases the amplitude of GABA_A mediated IPSPs in inhibitory neurons to a greater extent than the corresponding IPSPs in excitatory neurons. These results together with the theoretical predictions of Table I allow us to quantify such a difference.

By substituting median figures for ω^* before and after BZ administration (see Fig. 9) into Eqs. (5) and (6), we can obtain population estimates for ϵ and μ [BZ]. In this manner we find that $\epsilon \approx 1.8$ and $\mu\,[\mathrm{BZ}] \approx 1.6$, implying that the pharmacological properties of GABA_A receptors on inhibitory neurons are distinct from those on excitatory neurons. Thus for the average 1.36 Hz change in the median alpha pole frequency ($\Delta\omega^*$) following benzodiazepine administration, IPSPs in excitatory and inhibitory cells would have had their amplitude augmented by 1.6 and 2.9 times, respectively. It is worth noting that this predicted heterogeneity in the cellular distribution of GABA receptor subtypes is essentially independent of the characteristic spatial scale assumed for the alpha band activity, as can be determined by making additional calculations of ϵ for the different wave numbers of Table I.

It is well known that the heteropentameric GABA_A receptor can be classified into a number of subtypes depending upon either its pharmacological properties or subunit composition [40,41]. The majority of GABA_A receptors contain α, β, and γ subunits each of which has a number of specific isoforms, with the effects of benzodiazepines dependent on subunit composition in a complex manner. For example, a γ subunit is required for GABA_A benzodiazepine sensitivity,

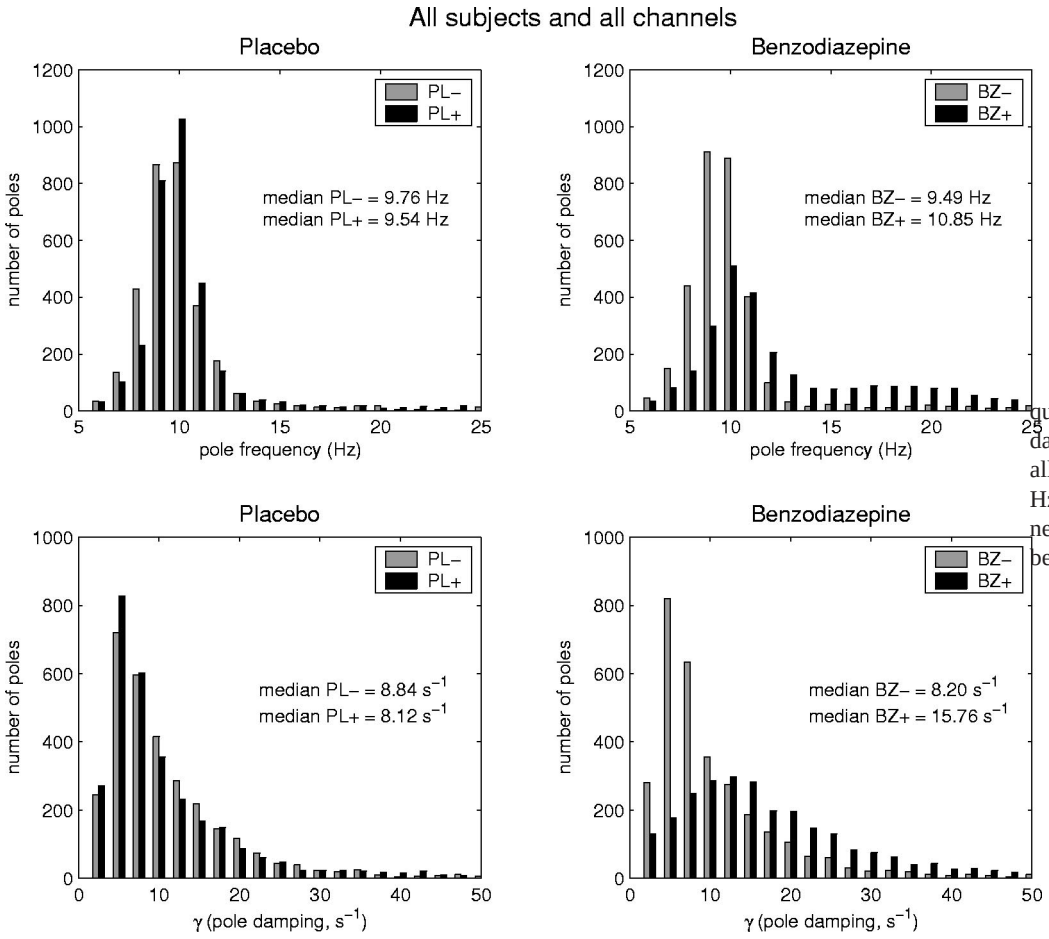

FIG. 9. Histograms of frequency (bin width=1 Hz) and damping (bin width=2.5 s^{-1}) for all poles lying between 6 and 30 Hz for all subjects and all channels for each of the placebo and benzodiazepine conditions.

the magnitude of which depends upon whether the γ_1 (low sensitivity), γ_2 (high sensitivity), or γ_3 (low sensitivity) isoform is present [42]. In addition, the nature of the α subunit (which has six known isoforms) comprising the $GABA_A$ receptor also determines BZ sensitivity [40]. The cellular distribution of the various receptor subtypes has been determined using *in situ* immunohistochemical methods and indicates that there is great diversity in their cellular distribution. Of particular relevance are the reports indicating the different subtype distribution expressed on pyramidal neurons ($\alpha_2\beta_3\gamma_2$-A2a3) and interneurons ($\alpha_1\beta_2\gamma_2$-A1a2) in rat hippocampus [43]. The latter subtype (an example of the

TABLE III. Comparisons between nonparametric (fast Fourier transform, FFT) and parametric methods [eighth-order autoregressive fifth-order moving average, (8,5) ARMA] for power spectral analysis. $\overline{\Delta f_c}$ is the mean change in the alpha center frequency and $\overline{\Delta\alpha}$ and $\overline{\Delta\beta}$ are the mean changes in fractional alpha (8–13 Hz) and beta (13–30 Hz) power, respectively, between benzodiazepine and placebo conditions. All p (significance) values were determined using a one-sided permutation test.

Channel	$\overline{\Delta f_c}$ (Hz)	p	$\overline{\Delta\alpha}$	p	$\overline{\Delta\beta}$	p
			48 ($n=14$)			
FFT	0.698	0.178	−0.142	0.0022	0.110	0.00012
ARMA	−0.523	0.325	−0.126	0.0024	0.115	0.00006
			50 ($n=14$)			
FFT	1.570	0.036	−0.125	0.0087	0.110	0.00018
ARMA	−2.214	0.0086	−0.113	0.0016	0.098	0.00006
			56 ($n=13$)			
FFT	0.419	0.309	−0.154	0.0061	0.085	0.0012
ARMA	−0.401	0.379	−0.149	0.0027	0.081	0.0021
			57 ($n=14$)			
FFT	0.209	0.369	−0.149	0.0080	0.094	0.0003
ARMA	−0.575	0.292	−0.136	0.0027	0.113	0.00018

type I BZ receptor) has high affinities and efficacies for a wide range of BZ agonists whereas the former (an example of the type II BZ receptor), while not fully characterized, is believed to have lower affinities and potencies [40]. Thus our prediction that alprazolam acts with greater effect at inhibitory→inhibitory synapses than inhibitory→excitatory is consistent with what is currently known about the distribution and molecular pharmacology of $GABA_A$ receptor subtypes. However, specific *in situ* immunohistochemical work is required regarding subtype distribution and alprazolam binding in order to confirm this. Because human data regarding subtype distribution are unlikely to be easily obtained, a preferable approach may be to look at genetic linkages between $\Delta\omega$ and $GABA_A$ receptor genes. In a recent study, Porjesz *et al.* [44] demonstrated a significant linkage for EEG frequencies in the β band (13–30 Hz) and a cluster of $GABA_A$ receptor genes located on chromosome 4.

If more detailed studies of the type outlined here are performed involving sedation measures (critical flicker fusion [45], choice reaction task [46], and the line analog rating scale [47]), then quantitative relationships can be established between pole motion and the level of sedation. Ultimately this would pave the way for the development of more reliable and rational methods for the assessment of sedation in the clinical setting, as is needed during short term anesthesia. Further, because the theory does not need to specify how bulk cortical inhibitory neurotransmission is modified, the theoretically constrained ARMA modeling described here is applicable to investigating the physiological effects and mechanisms of a wide range of centrally acting pharmaceuticals. Such compounds include general anesthetics and barbiturates, which are known to alter the shape and amplitude of the unitary IPSP. In addition to quantifying cortical GABAergic modulations, our method can be used to investigate the normative spatial (via the topographic mapping of r and θ) and temporal (longitudinal pole stability) structure of the human alpha rhythm. On this basis, fixed order ARMA modeling can be used to further elaborate and quantify developmental changes in the alpha rhythm that are known to occur [48], thus enabling greater insight into the genesis of this ubiquitous and important cortical rhythm.

APPENDIX A: CANONICAL ELECTROCORTICAL EQUATIONS

The theory of alpha electrorhythmogenesis is based upon a detailed spatially continuous two-dimensional mean field theory of electrocortical activity [7–9]. The principal state variables modeled are the mean soma membrane potentials of local cortical populations of excitatory and inhibitory neurons. The local field potential, and hence the EEG/ECOG, is regarded as being linearly related to the mean soma membrane potential of the excitatory neurons h_e. This theory can be cast as a set of coupled nonlinear one-dimensional partial differential equations that incorporate the major bulk anatomical and physiological features of cortical neurons and include cable delays, neurotransmitter kinetics, and intracortical and excitatory cortico-cortical connectivities. The spontaneous alpha rhythm is theorized to arise predominantly as a consequence of the local linear properties of cortex. For this reason in the current formulation spatial effects have been restricted to one dimension:

$$\tau\frac{\partial h(x,t)}{\partial t}=h^{\text{rest}}-h(x,t)+\Psi_e(h)I_e(x,t)+\Psi_i(h)I_i(x,t), \tag{A1}$$

$$\left(\frac{\partial}{\partial t}+\gamma_e\right)^2 I_e(x,t)=\Gamma_e\gamma_e\exp(1)\times\{N_e^\beta S_e(h_e)+\phi(x,t)+p_e(x,t)\}, \tag{A2}$$

$$\left(\frac{\partial}{\partial t}+\gamma_i\right)^2 I_i(x,t)=\Gamma_i\gamma_i\exp(1)\{N_i^\beta S_i(h_i)+p_i(x,t)\}, \tag{A3}$$

$$\left(I\frac{\partial}{\partial t}+\overline{v}\Lambda\right)^2\phi(x,t)-\overline{v}^2\frac{\partial^2\phi(x,t)}{\partial x^2}=\overline{v}\Lambda N^\alpha\left(\overline{v}\Lambda+I\frac{\partial}{\partial t}\right)S_e(h_e), \tag{A4}$$

where $h=(h_e,h_i)^T$, $h^{\text{rest}}=(h_e^{\text{rest}},h_i^{\text{rest}})^T$, $I_e=(I_{ee},I_{ei})^T$, $I_i=(I_{ie},I_{ii})^T$, $N_e^\beta=(N_{ee}^\beta,N_{ei}^\beta)^T$, $N_i^\beta=(N_{ie}^\beta,N_{ii}^\beta)^T$, $N^\alpha=(N_{ee}^\alpha,N_{ei}^\alpha)^T$, $\phi=(\phi_e,\phi_i)^T$, $\Lambda=\text{diag}(\Lambda_{ee},\Lambda_{ei})$, $\tau=\text{diag}(\tau_e,\tau_i)$, $\Psi_j(h)=\text{diag}(\psi_j(h_e),\psi_j(h_i))$, $p_e=(p_{ee},p_{ei})^T$, $p_i=(p_{ie},p_{ii})^T$, and I is the identity matrix, with

$$S_j(h_j)=S_j^{\max}\{1+\exp[-\sqrt{2}(h_j-\overline{\mu}_j)/\hat{\sigma}_j]\}^{-1}, \tag{A5}$$

$$\psi_{j'}(h_j)=(h_{j'}^{\text{eq}}-h_j)/|h_{j'}^{\text{eq}}-h_j^{\text{rest}}|, \tag{A6}$$

where $j,j'=e,i$. $S_j(h_j)$ represents the mean firing rates of neurons of type j. Thus oscillatory activity in the EEG, as represented by $h_e(t)$, implies oscillatory activity in the mean excitatory neuron firing rate $S_e(h_e(t))\equiv S_e(t)$. Table IV defines all the theoretical parameters and indicates the ranges that are used to generate parameter sets that give rise to stable physiological alpha activity.

The unitary IPSP and EPSP correspond to the perturbation in the mean soma membrane potential, of a postsynaptic neuron, induced by a *single* presynaptic action potential that arises from an inhibitory and excitatory neuron, respectively.

In the current theory an average IPSP ($j'=i$) or EPSP ($j'=e$) corresponds to the solution of the reduced equations

$$\tau_j\frac{dh_j}{dt}=h_j^{\text{rest}}-h_j+\psi_{j'}(h_j)I_{j'j}, \tag{A7}$$

$$\left(\frac{d}{dt}+\gamma_{j'}\right)^2 I_{j'j}=\Gamma_{j'}\gamma_{j'}\exp(1)\delta(t), \tag{A8}$$

where

$$h_j(0)=h_j^{\text{rest}},\quad I_{j'j}(0)=\dot{I}_{j'j}(0)=0.$$

Note that Eqs. (A7) and (A8) imply that the shape of both IPSPs and EPSPs are described by a third-order differential

TABLE IV. Numerical values of all anatomical and physiological parameters used in the generation of electroencephalographically plausible alpha activity. The ranges refer to the intervals from which uniform parameter deviates were generated.

Symbol	Definition	Typical value	Range	Units
e, i	Excitatory, inhibitory			
h_e, h_i	Mean soma membrane potential of e and i neurons			
h_e^{rest}, h_i^{rest}	Mean resting membrane potential	-60, -60		mV
h_e^{eq}, h_i^{eq}	Mean reversal potential associated with excitation or inhibition	0, -70		mV
N_{ee}^{α}, N_{ei}^{α}	Mean total number of connections that a cell of type e,i receives from excitatory cells via cortico-cortical fibers	4000, 2000	2000–5000, 1000–3000	
N_{ee}^{β}, N_{ei}^{β}	Mean total number of connections that a cell of type e,i receives from excitatory cells via intracortical fibers	3034, 3034	2000–5000, 2000–5000	
N_{ie}^{β}, N_{ii}^{β}	Mean total number of connections that a cell of type e,i receives from inhibitory cells	536, 536		
τ_e, τ_i	Effective passive membrane time constant	0.01, 0.01	0.005–0.15, 0.005–0.15	s
$\kappa=\Lambda_{ee}=\Lambda_{ei}$	Characteristic scale of $e\rightarrow e$, $e\rightarrow i$ cortico-cortical fibers	0.4	0.1–1.0	cm^{-1}
v	Mean cortico-cortical conduction velocity	700	1–1000	$\mathrm{cm\,s}^{-1}$
Γ_e, Γ_i	Effective excitatory, inhibitory postsynaptic potential peak amplitude	0.4, 0.8	$-$, 0.1–2	mV
γ_e, γ_i	Effective excitatory, inhibitory postsynaptic potential rate constant	300, 65	100–500, 10–200	s^{-1}
$\overline{\mu_e}$, $\overline{\mu_i}$	Excitatory, inhibitory population thresholds	-50, -50	-60–0, -60–0	mV
$S_e^{\max}$, $S_i^{\max}$	Excitatory, inhibitory population mean maximal firing rates	100, 100		Hz
p_{ee}, p_{ei}	Excitatory input to excitatory, inhibitory cells	0, 0		Hz
p_{ie}, p_{ii}	Inhibitory input to excitatory, inhibitory cells	0, 0		Hz
$\hat{\sigma}_e$, $\hat{\sigma}_i$	Standard deviation for firing threshold in excitatory, inhibitory populations	5, 5		mV

equation. The theoretically assumed shape of these postsynaptic potentials accords well with experiment [49]. It is important to emphasize that details of the neuronal dendritic cable properties and neurotransmitter kinetics are subsumed into the parameters τ_j, γ_j, and Γ_j. For this reason we refer to τ_j, γ_j, and Γ_j as the *effective* passive membrane time constant, PSP rate constant, and PSP peak amplitude respectively. It is experimentally well established that the amplitude of the unitary IPSP [1] (which is determined by Γ_i) is augmented in the presence of extracellular benzodiazepines. In the current theory it has not been necessary to assume any functional form for $\Gamma_i([\mathrm{BZ}])$ other than it is a monotonically increasing function of the extracellular benzodiazepine levels ([BZ]), because of the subsequent linear sensitivity analysis. Figure 3 shows an IPSP obtained from the solution of Eqs. (A7) and (A8) and the theoretically assumed effect of extracellular benzodiazepines on its amplitude.

In order to determine theoretically whether the alpha rhythm can be understood in terms of a white noise fluctuation spectrum, the above equations are linearized about spatially homogeneous singular points. For a given set of parameters these singular points can be obtained by setting all spatial and temporal derivatives to zero and solving for h_e. In general, these singular points h_e^* are solutions to

$$F(h_e(q),q)=0, \tag{A9}$$

where q represents a vector of model parameters and $F(\cdot)$ is obtained from Eqs. (A1)–(A4).

Linearizing Eqs. (A1)–(A4) about the spatially homogeneous singular point h_e^* and transforming to the Fourier domain [8] yields

$$H_e(k,\omega)=\frac{\exp(1)\Gamma_e\gamma_e\eta_e}{\tau_e}\,\frac{N(k,\omega;q)}{D(k,\omega;q)}P(k,\omega) \tag{A10}$$

$$=G_e(k,\omega;q)P(k,\omega), \tag{A11}$$

where

$$N(k,\omega)=\{(i\omega+\gamma_i)^2(i\omega+\eta_i/\tau_i) - w_{ii}N_{ii}^{\beta}Q_i\}\{(\kappa+i\omega/v)^2+k^2\}, \tag{A12}$$

$$\begin{aligned}D(k,\omega)=&\{(i\omega+\gamma_i)^2(i\omega+\eta_i/\tau_i)-w_{ii}N_{ii}^{\beta}Q_i\}\\&\times(\{(\kappa+i\omega/v)^2+k^2\}(i\omega+\eta_e/\tau_e)(i\omega+\gamma_e)^2\\&-w_{ee}Q_e[N_{ee}^{\alpha}\kappa(\kappa+i\omega/v)+N_{ee}^{\beta}\{(\kappa+i\omega/v)^2\\&+k^2\}])-w_{ei}w_{ie}N_{ie}^{\beta}Q_eQ_i[N_{ei}^{\alpha}\kappa(\kappa+i\omega/v)\\&+N_{ei}^{\beta}\{(\kappa+i\omega/v)^2+k^2\}],\end{aligned} \tag{A13}$$

$$w_{j'j}=\exp(1)\Gamma_{j'}\gamma_{j'}\eta_{j'}\psi_{j'}(h_j^*)/(\tau_{j'}\eta_j), \tag{A14}$$

$$\eta_j = 1 + \exp(1)\Gamma_e(N_{ej}^{\alpha} + N_{ej}^{\beta})S_e(h_e^*)/(\gamma_e|h_e^{\mathrm{eq}} - h_j^{\mathrm{rest}}|) + \exp(1)\Gamma_i N_{ij}^{\beta} S_i(h_i^*)/(\gamma_i|h_i^{\mathrm{eq}} - h_j^{\mathrm{rest}}|), \tag{A15}$$

$$Q_j = \partial S_j / \partial h_j|_{h_j = h_j^*}, \tag{A16}$$

where for simplicity $\kappa = \Lambda_{ee} = \Lambda_{ei}$, G_e is the *electrocortical transfer function*, and h_i^* can always be written as a function of h_e^*, i.e., $h_i^* = h_i(h_e^*)$ [see Eq. A1)]. $H_e(k,\omega)$ is defined as

$$H_e(k,\omega) = \int_{-\infty}^{\infty}\int_{-\infty}^{\infty} dx\, dt\, h_e(x,t)\exp(-i\omega t)\exp(-ikx). \tag{A17}$$

The roots ω^* found by solving $D(k,\omega;q)=0$ for fixed real k give the theoretically predicted EEG resonant frequencies ω^*, under the assumption that cortical input is so complicated as to be indistinguishable from white noise. For stable oscillatory behavior [i.e., all $-\mathrm{Im}(\omega^*)<0$], it is found that of the eight roots only a conjugate pair near the origin remain weakly damped under widespread parametric variation. This pair of roots (or poles) will dominate the linear behavior of the model. No analytical expressions can be obtained for the functional dependence of these weakly damped roots on model parameters. However, by performing a Monte Carlo parameter space search, assuming all parameters are uniformly distributed on the intervals given in Table IV, it is established that electroencephalographically and parametrically plausible alpha activity (as determined from the most weakly damped root over all k: $-\mathrm{Im}(\omega^*)<0$, $16\pi \leqslant |\mathrm{Re}(\omega^*)| \leqslant 26\pi$ rad s^{-1} and $|\mathrm{Re}(\omega^*)|/[2\,\mathrm{Im}(\omega^*)] \geqslant 5$) is widespread. The sensitivity of these model resonances to small perturbations in one or more of the model parameters q can be determined as follows. Rewriting the dispersion relationship $D(k,\omega;q)=0$ to depend explicitly upon h_e^* and q we get

$$D(k,\omega(q),h_e^*(q),q)=0. \tag{A18}$$

For any arbitrary parameter q_j of q the total derivative of D with respect to q_j is, by the chain rule,

$$\frac{\delta D}{\delta q_j} = \frac{\partial D}{\partial \omega}\frac{\partial \omega}{\partial q_j} + \frac{\partial D}{\partial h_e^*}\frac{\partial h_e^*}{\partial q_j} + \frac{\partial D}{\partial q_j} = 0. \tag{A19}$$

However, from Eq. (A9)

$$\frac{\delta F}{\delta q_j} = \frac{\partial F}{\partial h_e^*}\frac{\partial h_e^*}{\partial q_j} + \frac{\partial F}{\partial q_j} = 0, \tag{A20}$$

and, by combining Eqs. (A19) and (A20), it is found that

$$\frac{\partial \omega^*}{\partial \hat{q}_j} = q_j^*\left(\frac{\partial D}{\partial h_e^*}\frac{\partial F}{\partial q_j} - \frac{\partial D}{\partial q_j}\frac{\partial F}{\partial h_e^*}\right) \Big/ \left.\frac{\partial F}{\partial h_e}\frac{\partial D}{\partial \omega}\right|_{\omega^*, q^*}, \tag{A21}$$

where h_e^* is a solution of $F(h_e, q^*)=0$, ω^* is a solution of $D(k,\omega;q^*)=0$, q^* is the parameter set about which the sensitivity is calculated, and the $\hat{q}_j$ represent normalized parameters defined as $\hat{q}_j = (q_j - q_j^*)/q_j^*$.

$\partial\omega^*/\partial\hat{q}_j$ is the normalized local sensitivity of the root ω^* with respect to $\hat{q}_j$. In general, this quantity will be complex with $\partial\,\mathrm{Re}(\omega^*)/\partial\hat{q}_j\Delta\hat{q}_j$ and $-\partial\,\mathrm{Im}(\omega^*)/\partial\hat{q}_j\Delta\hat{q}_j$ giving the change in angular frequency and damping, respectively, of the root ω^* for a change in $\hat{q}_j$ of $\Delta\hat{q}_j$. The evaluation of the expressions in Eq. (A21) is most easily performed using a computerized symbolic algebraic system.

Thus the predicted change in the EEG resonant frequency, $\Delta\omega^*$, for *small* normalized (i.e., fractional) changes in the parameters, $\Delta\hat{q}_j$, is given simply by

$$\Delta\omega^* = \sum_j \frac{\partial \omega^*}{\partial \hat{q}_j}\Delta\hat{q}_j. \tag{A22}$$

APPENDIX B: SINGLE ELECTRODE ELECTROCORTICAL ARMA MODEL

Based on the white noise driving assumption of Appendix A the EEG recorded from a single electrode is modeled as

$$H_e(\omega) = \int_{-\infty}^{\infty} H_e(k,w)\Psi(k)dk, \tag{B1}$$

where $\Psi(k)$ is a *point spread function* that takes into account the finite conductivities of the skull and cerebrospinal fluid as well as the geometry of the recording electrode. In general, $\Psi(k)$ will act as a low-pass wave number filter. We will assume, with no subsequent loss of generality, that

$$\Psi(k) = \begin{cases} 1, & |k| \leqslant k_c \approx \pi/R, \\ 0 & \text{otherwise}, \end{cases} \tag{B2}$$

where R is the radius of a recording electrode. We choose $R \approx 0.25$ cm and thus $k_c \approx 6$ rad cm^{-1}. By rewriting $H_e(k,\omega)$ as

$$H_e(k,\omega) = \frac{\alpha(\omega) + \beta(\omega)k^2}{\gamma(\omega) + \delta(\omega)k^2}, \tag{B3}$$

where

$$\alpha = N(0,\omega),$$

$$\beta = \frac{1}{2}\frac{\partial^2 N(k,\omega)}{\partial k^2},$$

$$\gamma = D(0,\omega),$$

$$\delta = \frac{1}{2}\frac{\partial^2 D(k,\omega)}{\partial k^2},$$

a $\hat{k}(\omega)$ can be found such that

$$\frac{\alpha(\omega) + \beta(\omega)\hat{k}(\omega)^2}{\gamma(\omega) + \delta(\omega)\hat{k}(\omega)^2} = \int_0^{k_c} H_e(k,w)\Psi(k)dk. \tag{B4}$$

For the randomly generated parameter sets of Appendix A it is found that in the majority of cases (>80%) $\hat{k}(\omega) \propto \mathrm{Re}(\omega)$ and spans a relatively narrow range of wave numbers ($0.2-0.6\ \mathrm{rad\,cm^{-1}}$, median $=0.4\ \mathrm{rad\,cm^{-1}}$) over the range of electroencephalographic interest (0–30 Hz). Because $\hat{k}(\omega)=O(\omega)$ and $\beta(\omega)$ and $\delta(\omega)$ are $O(\omega^3)$ and $O(\omega^5)$, respectively, we are able to set $k=0.4\ \mathrm{rad\,cm^{-1}}$ in Eqs. (3) and (4).

[1] J.W. Gibbs, Y.F. Zhang, C.Q. Kao, K.L. Holloway, K.S. Oh, and D.A. Coulter, J. Neurophysiol. **75**, 1458 (1996).
[2] K. Kaila, Prog. Neurobiol. **42**, 489 (1994).
[3] M. Eghbali, J.P. Curmi, B. Birnir, and P.W. Gage, Nature (London) **388**, 71 (1997).
[4] R.J. Bertz, P.D. Kroboth, F.J. Kroboth, I.J. Reynolds, F. Salek, C.E. Wright, and R.B. Smith, J. Pharmacol. Exp. Ther. **281**, 1317 (1997).
[5] L.T. Breimer, P.J. Hennis, A.G. Burm, M. Danhof, J.G. Bovill, J. Spierdijk, and A.A. Vletter, Clin. Pharmacokinet. **18**, 245 (1990).
[6] M.A. Hotz, R. Ritz, L. Linder, G. Scollo-Lavizzari, and W.E. Haefeli, Br. J. Clin. Pharmacol. **49**, 72 (1999).
[7] D.T.J. Liley, in *Spatiotemporal Models in Biological and Artificial Systems*, edited by F.L. Silva, J.C. Príncipe, and L.B. Almeida (IOS Press, Amsterdam, 1997), pp. 89–96.
[8] D.T.J. Liley, P.J. Cadusch, and M.P. Dafilis, Network Comput. Neural Syst. **13**, 67 (2002).
[9] D.T.J. Liley, P.J. Cadusch, and J.J. Wright, Neurocomputing **26-27**, 795 (1999).
[10] M.L. Steyn-Ross, D.A. Steyn-Ross, J.W. Sleigh, and D.T.J. Liley, Phys. Rev. E **60**, 7299 (1999).
[11] M.P. Dafilis, D.T.J. Liley, and P.J. Cadusch, Chaos **11**, 474 (2001).
[12] M.A. Arbib, P. Érdi, and J. Szentágothai, *Neural Organization*: *Structure*, *Function and Dynamics* (MIT Press, Cambridge, MA, 1998).
[13] R. Llinás, Science **242**, 1654 (1988).
[14] M. Steriade, P. Gloor, R. Llinás, F.H. Lopes da Silva, and M.M. Mesulam, Electroencephalogr. Clin. Neurophysiol. **76**, 481 (1990).
[15] W.J. Freeman, *Mass Action in the Nervous System* (Academic Press, New York, 1975).
[16] W.J. Freeman, in *Induced Rhythms of the Brain*, edited by E. Başar and T.H. Bullock (Birkhauser, Basel, 1991), pp. 200–232.
[17] A. Rotterdam, F.H. Lopes da Silva, J. van der Ende, M.A. Viergever, and A.J. Hermans, Bull. Math. Biol. **44**, 283 (1982).
[18] H.R. Wilson and J.D. Cowan, Kybernetik **13**, 55 (1973).
[19] V.K. Jirsa and H. Haken, Phys. Rev. Lett. **77**, 960 (1996).
[20] P.L. Nunez, *Neocortical Dynamics and Human EEG Rhythms* (Oxford University Press, New York, 1995).
[21] P.L. Nunez, Behav. Brain Sci. **23**, 371 (2000).
[22] P.L. Nunez, Brain Topogr **1**, 199 (1989).
[23] P.A. Robinson, C.J. Rennie, and J.J. Wright, Phys. Rev. E **56**, 826 (1997).
[24] P.L. Nunez, *Electric Fields of the Brain*: *The Neurophysics of EEG* (Oxford University Press, New York, 1981).
[25] R.D. Traub, J.G.R. Jefferys, and M.A. Whittington, *Fast Oscillations in Cortical Circuits* (MIT Press, Cambridge, MA, 1999).
[26] W.J. Freeman, Sci. Am. **264** (2), 78 (1991).
[27] F.H. Lopes da Silva, A. Hoeks, H. Smits, and L.H. Zetterberg, Kybernetik **15**, 27 (1974).
[28] J.W. Prast, Electroencephalogr. Clin. Neurophysiol. **1**, 370 (1949).
[29] *Handbook for Digital Signal Processing*, edited by S.K. Mitra and J.F. Kaiser (Wiley-Interscience, New York, 1993).
[30] A. Destexhe, D. Contreras, T.J. Sejnowski, and M. Steriade, J. Neurophysiol. **72**, 803 (1994).
[31] M. Steriade and R. Llinás, Physiol. Rev. **68**, 649 (1988).
[32] P.A. Robinson, C.J. Rennie, J.J. Wright, H. Bahramali, E. Gordon, and D.L. Rowe, Phys. Rev. E **63**, 021903 (2001).
[33] P.A. Robinson, P.N. Loxley, S.C. O'Connor, and C.J. Rennie, Phys. Rev. E **63**, 041909 (2002).
[34] R.D. Traub and R. Miles, *Neuronal Networks of the Hippocampus* (Cambridge University Press, Cambridge, England, 1991).
[35] J.W. McAuley and C.I. Friedman, J. Clin. Psychopharmacol. **19**, 233 (1999).
[36] M.A. Wilson, Crit. Rev. Neurobiol. **10**, 1 (1996).
[37] P.M.T. Broersen, IEEE Trans. Signal Process. **48**, 2454 (2000); http://www.tudelft.nl/mmr
[38] P.M.T. Broersen, IEEE Trans. Instrum. Meas. **51**, 211 (2002).
[39] P.I. Good, *Permutation Tests*: *A Practical Guide to Resampling Methods for Testing Hypotheses*, Springer Series in Statistics (Springer-Verlag, New York, 2000).
[40] E.A. Barnard, P. Skolnick, R.W. Olsen, H. Mohler, W. Sieghart, G. Biggio, C. Braestrup, A.N. Bateson, and S.Z. Langer, Pharmacol. Rev. **50**, 291 (1998).
[41] E. Costa, Annu. Rev. Pharmacol. Toxicol. **38**, 321 (1998).
[42] M. Chebib and G.A.R. Johnston, J. Med. Chem. **43**, 1429 (2000).
[43] H. Mohler, J.M. Fritsschy, B. Lüscher, U. Rudolph, and J. Benson, in *Ion Channels*, edited by T. Narahashi (Plenum Press, New York, 1996), Vol. 4, pp. 89–113.
[44] B. Porjesz *et al.*, Proc. Natl. Acad. Sci. U.S.A. **19**, 3729 (2002).
[45] N. Sherwood and J. S. Kerr, in *Human Psychopharmacology*: *Measures and Methods*, Vol. 4, edited by I. Hindmarch and P. D. Stonier (Wiley, London, 1993).
[46] I. Hindmarch, Adv. Human. Psychopharmacol. **2**, 99 (1981).
[47] R.B.C. Atkin, Proc. R. Soc. Med. **62**, 989 (1969).
[48] R. Srinivasan, J. Clin. Neurophysiol. **110**, 1351 (1999).
[49] R. Miles and J.C. Poncer, Curr. Opin. Neurobiol. **6**, 387 (1996).